RESEARCH ARTICLE
doi.org/10.1002/elsa.202100198

Chemistry Europe
European Chemical Societies Publishing

Received: 8 November 2021
Revised: 20 December 2021
Accepted: 21 December 2021

Conversion of a CO–CO_2 co-feed with a porous tubular copper catalyst at low potential

Anne Clara Sustronk[1,2] | **Nieck Edwin Benes**[1] | **Guido Mul**[2]

[1] Films in Fluids, Faculty of Science and Technology, MESA+ Institute of Nanotechnology, University of Twente, AE Enschede, The Netherlands

[2] PhotoCatalytic Synthesis group, Faculty of Science and Technology, MESA+ Institute of Nanotechnology, University of Twente, AE Enschede, The Netherlands

Correspondence
G. Mul, PhotoCatalytic Synthesis group, Faculty of Science and Technology, MESA+ Institute of Nanotechnology, University of Twente, P.O. Box 217, 7500 AE Enschede, The Netherlands.
Email: g.mul@utwente.nl

Abstract

In the electrochemical reduction of CO_2, copper electrodes are well known to be active and selective for a variety of products, depending on process conditions. However, the effect of feed composition on performance has not been extensively investigated, especially with respect to the conversion of CO_2 to CO. We now show for copper electrodes in a porous tubular configuration (Hollow Fibre Electrodes, HFEs) at a relatively low working potential (−1.1 V vs Ag/AgCl), that an increasing concentration of CO in the feed results in a decreasing CO_2 conversion rate to CO. Contrary, it is observed that the concomitant hydrogen production rate does not depend on the concentration of CO in the feed. These observations are in good agreement with thermodynamic predictions applying the equation for the Gibbs energy of reaction. On the basis of this conclusion, we anticipate that mass transfer limitations are minimized by the tubular morphology and flow-through mode of operation. Most importantly, this study shows the necessity of a low CO concentration in the feed, to obtain a high CO_2 conversion rate.

KEYWORDS
co-feed, convective reactant supply, copper hollow fiber electrode, copper, electrochemical CO conversion, electrochemical CO2 conversion

1 | INTRODUCTION

Product accumulation in the vicinity of a heterogeneous electrocatalyst is common in electrochemistry.[1] This accumulation originates from mass transfer limitations in the boundary layer near the catalyst. The extent of accumulation depends on the reaction rate, the thickness of the boundary layer, and the rate of mass transfer. For example, a fast reaction rate, combined with slow mass transfer and a thick boundary layer, results in a high concentration of products in the vicinity of the surface of the electrode. In contrast, the concentration of products near the surface is low in the case of fast mass transfer, and a thin boundary layer.

During electrochemical CO_2 conversion over Cu electrodes, hydroxide ions and carbon monoxide (CO) accumulate in the vicinity of the catalyst surface, in particular at high current density. The accumulation of hydroxide ions increases the pH locally[2–5] and is said to benefit the ethylene production rate.[6] However, accumulation of hydroxide ions also results in a loss of reactant, as a result of a reaction between CO_2 and OH^- into (bi)carbonate.[2,4,5] With respect to the accumulation of CO in the vicinity of the electrode, knowledge is composed of studies that focus

RESEARCH ARTICLE
doi.org/10.1002/elsa.202100198
Chemistry Europe
European Chemical Societies Publishing

on the production of hydrocarbons.[7–9] It is reported, for example, that co-feeding CO and CO_2 improves the ethylene production rate.[7] Additionally, other research on the effect of surface concentration of reactants, products, and intermediates mainly focuses on the production of hydrocarbons (e.g., refs. [10,11]).

As far as we know, no studies have yet been reported on the effect of CO accumulation in the vicinity of an electrocatalyst on the conversion of CO_2 to CO. This topic is of interest for two reasons. First, industrial implementation of electrochemical CO_2 to CO conversion requires much higher current densities than commonly studied.[12] In case the CO production rate exceeds the rate at which CO is removed from the surface, accumulation of CO in the vicinity could lead to competitive adsorption of CO, inhibiting CO_2 conversion. Second, industrial implementation of electrochemical CO_2 conversion includes treatment of off-gasses that not only contain CO_2, but also contain other components such as CO.[13] If the presence of CO limits the CO_2 to CO conversion rate, additional measures are required to obtain a high conversion rate.

This work elucidates the effect of CO concentration on the electrochemical CO_2 conversion rate at low potential (−1.1 V vs Ag/AgCl). We studied this effect using tubular porous copper electrodes. These are distinct from the commonly used flat sheet electrodes based on their geometry and reactant supply method. In the case of flat sheet electrodes, CO_2 is commonly supplied through the electrolyte or at the back of the gas diffusion electrode.[14] In the case of tubular electrodes used in this research, CO_2 is supplied through the porous wall of the tubular electrode.[15] It is believed that flowing CO_2 through the porous wall benefits the CO_2 conversion rate. The so-called "copper hollow fibers" exhibit a selectivity of about 70% toward CO, 15% toward formate, and 15% toward H_2.[15] To study the effect of the presence of CO on the CO_2 conversion rate, we subjected the copper hollow fibers to CO-CO_2 feed compositions with various amounts of CO. Both the single-pass CO_2 conversion rate and the product distribution are reported and discussed.

2 | EXPERIMENTAL

2.1 | Copper hollow fiber preparation

The copper hollow fibers were prepared using the non-solvent induced separation method followed by thermal treatment. Twenty-eight grams of polyetherimide (PEI, Ultem1000) was dried at 110°C overnight. Two hundred eighty-four grams copper powder (1 μm, 99.8% SkySpring Nanomaterials) was added to 88.6 g 1-methyl-2-pyrrolidone (NMP, anhydrous, ≥99.5%, Sigma–Aldrich) and subsequently subjected to ultrasonic treatment for 30 min. Afterward, the PEI was added in two batches to the copper–NMP mixture with 30 min in between, while the mixture was stirred and heated in a water bath at 60°C. Stirring and heating continued until the polymer was dissolved. The mixture was allowed to cool down overnight while overhead stirring continued. The next day, the mixture was transferred to a pressure vessel and a vacuum was applied for 30 min. The vessel was left under vacuum overnight. Subsequent spinning occurred at ambient conditions, using a spinneret with an outer diameter of 2.0 mm and an inner diameter of 0.8 mm and 1 bar N_2 on the pressure vessel. Demi-water acted as both the bore liquid and precipitation bath. The air gap was set at 1 cm. After spinning, the fibers were left vertically to dry in the air, while applying a light stretch to the fibers. The thermal and H_2 treatment followed the same procedure as given by Kas et al.[15], except for the duration of the H_2 treatment. This duration was determined based on the weight of the CuO sample and the H_2 volumetric flow rate. The obtained copper hollow fibers were potted in a 6 mm SS Swagelok tube. Electrical connection was made with Ag glue (CircuitWorks CW2400). The glue was annealed for 10 min at 100°C in air. Next, the Ag glue connection was covered with epoxy glue (Araldite 2012). Also the bottom of the fiber was sealed with epoxy glue. The geometric area available was approximately 2.0 cm,[2] which equals to a fiber length of about 4.0 cm.

2.2 | Electrochemical setup

A 0.3 M $KHCO_3$ (VWR, Analar Normapur) solution in Milliq water was prepared. The reaction vessel was rinsed with electrolyte and filled with 100 ml ± 1 ml electrolyte. The chamber separating the anode from the cathode, the Pt on Ti mesh counter electrode and the glass reactor were regularly cleaned with 1 M HNO_3. A Ag/AgCl (3 M NaCl) reference electrode was used. The anode and cathode were separated by a piece of Zirfon membrane. The fibers were dried with >4.5 barg Ar or N_2 after each experiment. An image of the setup can be found in the Supporting Information.

2.3 | Chronoamperometry and chronopotentiometry

Fresh and used fibers were tested at various N_2-CO and CO-CO_2 ratios. The feed flow contained 10 ml min^{-1} CO_2 and between 0.5 and 6 ml min^{-1} CO. N_2 was used as balance gas to keep the total flow rate at 20 ml min^{-1}. No pre-saturation of the electrolyte was applied. First,

RESEARCH ARTICLE
doi.org/10.1002/elsa.202100198

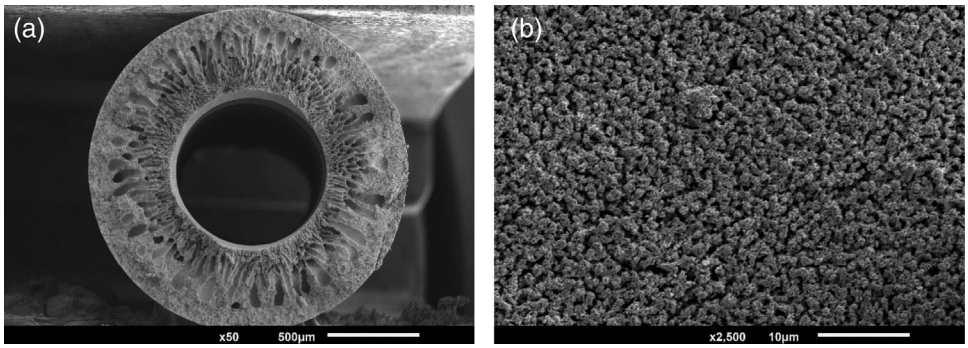

FIGURE 1 (a) Cross-section, (b) side view SEM image of copper hollow fiber

the internal resistance between work and reference electrode was measured by the current interrupt method. Subsequently, the system was allowed to relax for 2 min. Afterward, the chronoamperometry measurement was started at −1.1 V vs Ag/AgCl (about −0.45V vs RHE) and took 4 h. During the first hour of the chronoamperometry measurement, the sample was subjected to 30 vol% CO in N_2 or CO_2. During the second, third, and fourth hour of the chronoamperometry measurement, the CO concentration was changed with respect to the CO concentration of the previous hour. After the chronoamperometry measurement, another current interrupt measurement was performed to obtain the resistance between the work and reference electrode. Common resistance values for this setup were between 5 and 10 Ω. All data shown here are uncorrected for the internal resistance.

The gas phase was analyzed by means of GC analysis. The GC was equipped with an Rt-Q-bond and Shin Carbon micropacked column connected to a TCD for the detection of hydrogen, oxygen, CO, and CO_2. Additionally, the GC has an Rtx-1 column that was connected to the FID for the detection of hydrocarbons. The carrier gas was changed from helium to argon in the course of the research. The sampling time was 6 min with helium as carrier gas and 10 min with argon as the carrier gas.

The procedure of a chronopotentiometry experiment is equal to the procedure of a chronoamperometry experiment, except for the application of a constant current of −7.4 mA to the sample instead of a constant potential.

3 | RESULTS AND DISCUSSION

Figure 1a shows a cross section of a copper hollow fiber. The cross section is characterized by the macrovoids at the inside of the fiber, and a more dense porous layer near the outer wall. An interface at the outside of the fiber between CO_2, the copper hollow fiber, and the 0.3 M $KHCO_3$ electrolyte is established, as a result of CO_2 being supplied from the inside of the fiber. The active surface area at the outside of the fiber is characterized by its rough and porous structure and is shown in Figure 1b.

An example of a current response while feeding different amounts of CO to the fiber in the absence of CO_2 is given in Figure 2a. From the figure, it becomes apparent that the current significantly decreases during the first hour of chronoamperometry, followed by a small decrease during the remaining 3 h . Similar behavior is observed for two other samples and is presented in Figure S3. The sharp decrease in current in the first hour of the experiment is related to the conversion of a copper oxide layer on the outside of the fiber to metallic copper. This oxide layer origins from exposing the fibers to air while assembling the reactor.[16] The small activity decrease in the subsequent 3 h is related to the continued conversion of copper oxide to copper and surface reconstruction as a consequence of the presence of CO.[17–21] Figure 2a also shows that the current response is independent of the amount of CO present in the CO feed, suggesting CO is not reactive at the potential applied in the experiment.

GC analysis of the gaseous product stream confirms the absence of methane or other hydrocarbons, and thus reactivity of CO, and reveals that only H_2 is formed at the cathode. About 90% of the current can be accounted for in terms of H_2 production, as shown in Figure 2b. The same figure shows that the selectivity toward H_2 is independent of the CO feed concentration. The remaining 10% of the current is related to surface reconstruction, mainly reduction of the surface and sub-surface oxide and interaction between CO and the copper surface.[21]

Figure 3a shows the current response of a fiber subjected to a CO–CO_2 co-feed containing different amounts of CO. The figure indicates the same decrease in current during the first hour of chronoamperometry as was observed for the CO feed in the absence of CO_2. During the remaining 3 hour, the current responds according to the CO content in the feed. The current increases to more negative values when the CO content is decreased, and the current decreases to less negative value when the CO content is increased.

RESEARCH ARTICLE
doi.org/10.1002/elsa.202100198
Chemistry Europe
European Chemical Societies Publishing

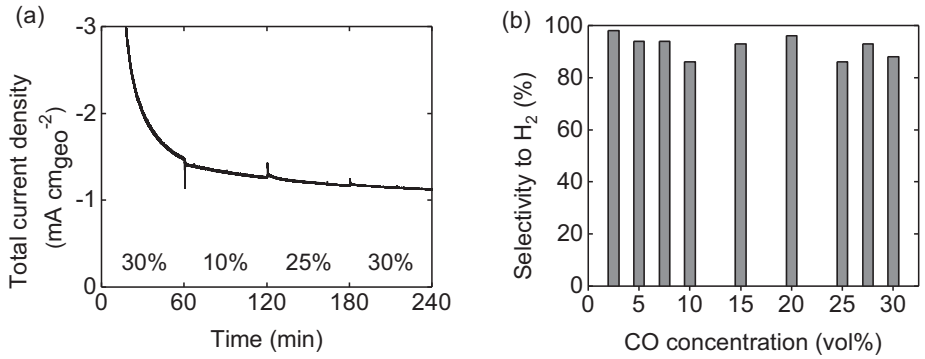

FIGURE 2 (a) Current response of 'Sample A' to several CO vol% in N_2-CO feed at −1.1 V vs Ag/AgCl; (b) Selectivity to H_2

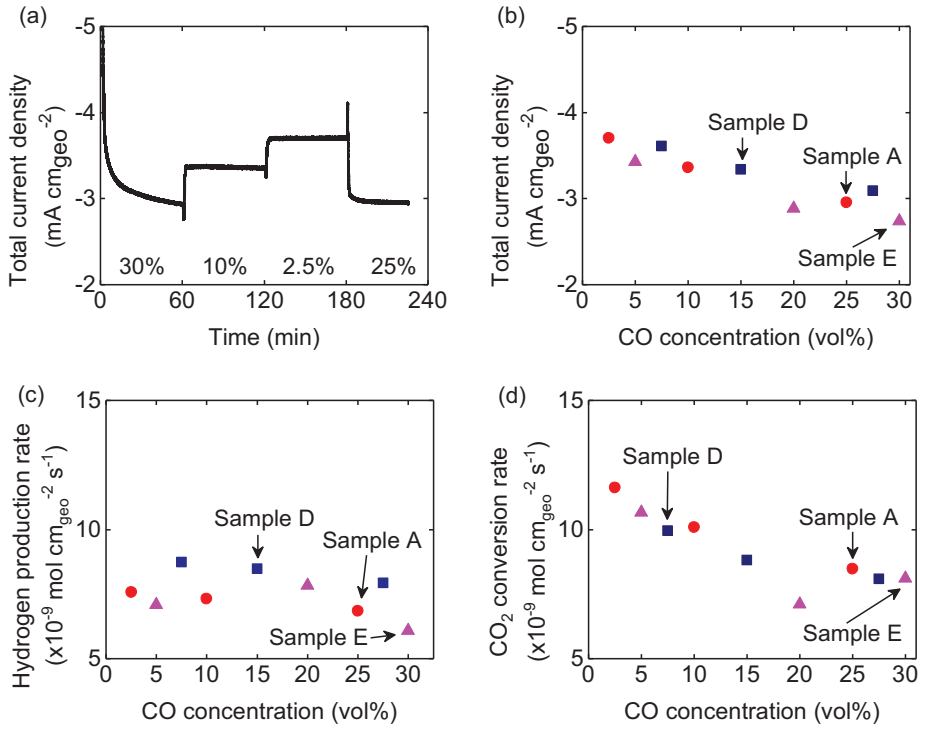

FIGURE 3 (a) Current response of 'Sample A' to several CO vol% in a CO-CO_2 co-feed at −1.1 V vs Ag/AgCl; (b) Overall catalyst activity; (c) H_2 production rate for several CO vol% in CO-CO_2 co-feed and (d) CO_2 conversion rate

The effect of CO on the total catalyst activity becomes more apparent when the CO concentration is plotted against the total current density. Figure 3b clearly shows that the catalyst activity decreases when the CO content increases. Here, we would like to emphasize that this decrease is the result of an increase in the CO content in the feed, as the experiment is designed to maintain a constant CO_2 (partial) pressure.

We elucidate the decrease in total catalytic activity as described by Figure 3b on the basis of the H_2 production rate and CO_2 conversion rate. From Figure 3c it becomes apparent that the H_2 production rate is independent of the CO feed concentration in the CO–CO_2 co-feed, similar to the observation of the pure CO feed (Figure 2b). This independence is confirmed by performing an *F*-test (99% confidence; see the Supporting Information for more information) and is also reported by Ooka et al.[22] On the other hand, the CO_2 conversion rate decreases with an increasing amount of CO in the CO–CO_2 co-feed, as shown in Figure 3d. As a result of the experimental method, we were only able to determine the CO_2 conversion rate and not the CO production rate. The amount of CO produced fell in the experimental error of the GC analysis. Nevertheless, Figure 3d clearly shows that the CO_2 conversion is lower in the presence of CO.

Then the question arises why the CO_2 conversion rate appears to be dependent on the presence of CO in the feed, while the hydrogen production rate appears to be

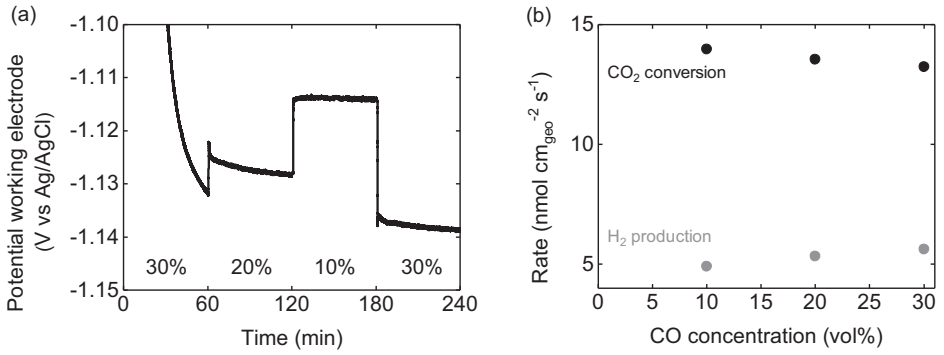

FIGURE 4 (a) Potential response for a current fixed at −7.4 mA of "Sample F" to several CO vol% in a CO–CO_2 co-feed; (b) CO_2 conversion rate and H_2 production rate

independent of the applied CO concentration. To answer these questions, we evaluate the observations on the basis of the Gibbs free energy of the electrochemical reaction and the corresponding potential required for the reaction to occur.[23] In case of the conversion of CO_2 into CO, the required potential becomes more negative in case CO is present in the reaction mixture (for example −0.770 V at 10 vol% CO and −0.784 V at 30 vol% CO, see the Supporting Information, Table S4). In other words, thermodynamically, more energy is required to convert CO_2 into CO, in case CO is present. However, the experimental working electrode potential was kept at a constant value. As a consequence, the driving force of the CO_2 conversion reaction, the overpotential (E_{WE} − E, in which E_{WE} is the potential at the working electrode, and E the thermodynamically determined potential), becomes smaller when the CO concentration in the feed is increased. The current and the CO_2 conversion rate decrease accordingly. On the other hand, the driving force for H_2 production remains constant, as CO is not involved in the Gibbs energy of H_2 evolution. This explains the observed constant H_2 production rate.

In addition to the interpretation of the data based on thermodynamics, we have considered the possibility of CO adsorption on active catalytic sites, inhibiting CO_2 conversion. If CO adsorption would be considerable, one would expect that the H_2 production rate would also respond to changes in CO partial pressure. However, Figures 2b and 3c indicate that the H_2 production rate is independent of the CO partial pressure. Furthermore, in the case of irreversible adsorption of CO, one would expect the current to attain different values if a sample is first subjected to a high CO partial pressure and subsequently to a low, or vice versa. Since the order in changing the CO concentration does not affect the results, this suggests that inhibition of catalytically active sites by CO adsorption, hardly plays a role, if any.

We will now address the effect of the concentration of CO on the potential at the working electrode, at constant current conditions. Figure 4a shows the relation between the CO feed content and the working potential, while the current is kept constant at −7.4 mA. As expected, the experimentally required voltage increases as a function of increasing CO concentration. However, it is not possible to directly relate the change in working potential to the CO_2 conversion rate, as both CO_2 conversion and H_2 production occur in the studied potential range. In fact, Figure 4b shows an increase in the H_2 production rate while the amount of CO in the feed (and the applied voltage) increases, while the CO_2 conversion rate decreases. To explain these trends, let us consider the effect of changing the CO concentration from 10% to 30%. This leads to an increase in the observed potential at the WE of approximately 15 mV (see Table S4). When the thermodynamic potentials for both reactions are considered, it becomes apparent that these 15 mVs can be divided into an overpotential for the CO_2 conversion reaction of approximately 5 mV, and an overpotential for H_2 formation of at least 10 mV (see Table S4). The larger fraction of the additional potential for H_2 formation, changes the ratio contributing to the overall constant current to respectively convert CO_2, or produce H_2. In other words, the Faradaic Efficiency for H_2 formation increases. These results underline the importance of considering the thermodynamic potential to explain the results.

The results presented here suggest that the CO_2 conversion rate is compromised by the presence of CO, largely determined by thermodynamics. Since the relative magnitude of the effect of CO concentration matches the predictions on the basis of thermodynamics so well, this suggests that mass transfer limitations are minimized, when the CO_2 is purged through the porous wall of the hollow fiber electrode. When CO is formed by the reduction of CO_2, our study implies there is a need for fast CO removal from the electrode surface, not to experience the consequences of thermodynamically induced higher potential requirements. In view of industrial implementation of electrochemical CO_2 to CO conversion, the results suggest that additional measures are required when the electrode is fed

with a mixture of CO and CO_2. Although a lower CO_2 conversion rate could be partially alleviated by applying a higher working potential, this approach results into a higher energy consumption, since the hydrogen production rate is significantly favored. Removal of CO from CO_2 prior to electrocatalytic conversion in the case of a CO_2–CO co-feed could limit the effect of CO on the CO_2 conversion rate. However, the required CAPEX and OPEX of membrane separation might be of concern.

4 | CONCLUSION

This study shows the effect of adding CO to CO_2 with respect to CO_2 conversion and hydrogen evolution, using porous, tubular copper electrodes acting as a working electrode. Knowing this effect is particularly important in terms of industrial implementation of electrochemical CO_2 to CO conversion, where industrial waste streams do not only contain CO_2, but also other components such as CO. The electrode was fed with different amounts of CO, while maintaining a constant CO_2 partial pressure. It was observed that the CO_2 conversion rate decreases with increasing CO feed content, whereas the H_2 production rate remains constant. The observed phenomena are in agreement with changes in overpotential determined on the basis of the Gibbs energy of reaction and the applied constant potential at the working electrode. The results indicate that industrial implementation of electrochemical CO_2 to CO conversion requires additional measures when targeting a CO–CO_2 co-feed.

ACKNOWLEDGMENTS
This research is financially supported with a subsidy from the Topsector Energy by the Dutch Ministry of Economic Affairs and Climate Policy and is conducted within the framework of the Institute of Sustainable Process Technology (project number SI-20-03).

CONFLICT OF INTEREST
The authors declare no conflict of interest

AUTHOR CONTRIBUTIONS
A.C.S. was associated with conceptualization, investigation, wrote the original draft, and visualization. N.E.B. and G.M. were associated with conceptualization, supervision, and reviewed and edited the final manuscipt.

DATA AVAILABILITY STATEMENT
The raw data is uploaded in the 4TU. ResearchData repository and will become available after publication of this article through https://doi.org/10.4121/16951180.

REFERENCES
1. D. Pletcher, *A First Course in Electrode Processes*, 2nd ed., RSC Publishing **2009**.
2. H. Hashiba, L.-C. Weng, Y. Chen, H. K. Sato, S. Yotsuhashi, C. Xiang, A. Z. Weber, *J. Phys. Chem. C* **2018**, *122*, 3719–3726.
3. K. Yang, R. Kas, W. A. Smith, *J. Am. Chem. Soc.* **2019**, *141*, 15891–15900.
4. J. Resasco, Y. Lum, E. Clark, J. Z. Zeledon, A. T. Bell, *ChemElectroChem* **2018**, *5*, 1064–1072.
5. S. Nitopi, E. Bertheussen, S. B. Scott, X. Liu, A. K. Engstfeld, S. Horch, B. Seger, I. E. L. Stephens, K. Chan, C. Hahn, J. K. Nørskov, T. F. Jaramillo, I. Chorkendorff, *Chem. Rev.* **2019**, *119*, 7610–7672.
6. H. Xiang, S. Rasul, K. Scott, J. Portoles, P. Cumpson, E. H. Yu, *J. CO2 Util.* **2019**, *30*, 214–221.
7. X. Wang, J. F. de Araújo, W. Ju, A. Bagger, H. Schmies, S. Kühl, J. Rossmeisl, P. Strasser, *Nat. Nanotechnol.* **2019**.
8. N. S. Romero Cuellar, C. Scherer, B. Kaçkar, W. Eisenreich, C. Huber, K. Wiesner-Fleischer, M. Fleischer, O. Hinrichsen, *J. CO2 Util.* **2020**, *36*, 263–275.
9. Y. Lum, J. W. Ager, *Nat. Catal.* **2019**, *2*, 86–93.
10. Y. C. Tan, K. B. Lee, H. Song, J. Oh, *Joule* **2020**, *4*, 1104–1120.
11. H. Song, J. T. Song, B. Kim, Y. C. Tan, J. Oh, *Appl. Catal., B* **2020**, *272*, 119049.
12. T. Burdyny, W. A. Smith, *Energy Environ. Sci.* **2019**, *12*, 1442–1453.
13. T. A. Aarhaug, A. P. Ratvik, *JOM* **2019**, *71*, 2966–2977.
14. Y. Zhong, S. Wang, M. Li, J. Ma, S. Song, A. Kumar, H. Duan, Y. Kuang, X. Sun, *Mater. Today Phys.* **2021**, *18*, 100354.
15. R. Kas, K. K. Hummadi, R. Kortlever, P. de Wit, A. Milbrat, M. W. J. Luiten-Olieman, N. E. Benes, M. T. M. Koper, G. Mul, *Nat. Commun.* **2016**, *7*, 10748.
16. A. Dutta, M. Rahaman, N. C. Luedi, M. Mohos, P. Broekmann, *ACS Catal.* **2016**, *6*, 3804–3814.
17. A. S. Malkani, M. Dunwell, B. Xu, *ACS Catal.* **2019**, *9*, 474–478.
18. Z. Sun, M. M. Sartin, W. Chen, F. He, J. Cai, Y. X. Chen, *J. Phys. Chem. C* **2019**, *123*, 21467–21477.
19. M. M. Sartin, Z. Yu, W. Chen, F. He, Z. Sun, Y. X. Chen, W. Huang, *J. Phys. Chem. C* **2018**, *122*, 26489–26498.
20. C. M. Gunathunge, V. J. Ovalle, Y. Li, M. J. Janik, M. M. Waegele, *ACS Catal.* **2018**, *8*, 7507–7516.
21. S. K. Shaw, A. Berná, J. M. Feliu, R. J. Nichols, T. Jacob, D. J. Schiffrin, *Phys. Chem. Chem. Phys.* **2011**, *13*, 5242–5251.
22. H. Ooka, M. C. Figueiredo, M. T. M. Koper, *Langmuir* **2017**, *33*, 9307–9313.
23. P. Atkins, J. de Paula, *Atkins' Physical Chemistry, Chapter 6 Chemical equilibrium*, 9th ed., Oxford University Press **2010**.

SUPPORTING INFORMATION
Additional supporting information may be found in the online version of the article at the publisher's website.

How to cite this article: A. C. Sustronk, N. E. Benes, G. Mul, *Electrochem Sci Adv*. **2022**, e2100198. https://doi.org/10.1002/elsa.202100198